PERGAMON

International Journal of Impact Engineering 26 (2001) 735–744

INTERNATIONAL JOURNAL OF IMPACT ENGINEERING

www.elsevier.com/locate/ijimpeng

THE SHAPED CHARGE JET INTERACTION WITH FINITE THICKNESS TARGETS

OLEG V. SVIRSKY, NICOLAI P. KOVALEV, BORIS A. KLOPOV, VADIM V. BASHUROV, and VICTOR A. KRUTYAKOV

Russian Federal Nuclear Center-VNIIEF, Sarov, Nizhnii Novgorod Region, 607190, RUSSIA

Abstract — The problem of reducing the jet penetration capability upon its interaction with the finite-thickness target, due to the erosion of the front region of the jet having perforated through the target, is considered. The experimental examination and the mathematical modeling of the process were performed; semi-empirical formulas were obtained. The calculation techniques are shown to allow the description of interaction processes with satisfactory accuracy. © 2001 Elsevier Science Ltd. All rights reserved.

Keywords: shaped charge, jet, target, foreshortening, erosion, perforating, penetration, tip velocity, standoff distance.

NOTATION

d_j	jet diameter
Δl	additional jet length erosion
V	jet tip velocity
V_t	jet tail velocity
B	virtual origin
Δ	target thickness
S	standoff distance
P	penetration
ρ	density
u	penetration velocity
FS	foreshortening (jet shortening due to radial erosion of its front region)
RHA	rolled homogenous armor
HE	high-energy explosives

INTRODUCTION

Notwithstanding considerable efforts made by many researchers and in spite of its great practical importance, the problem of calculation description of the shaped charge jet interaction with the target, still remains not studied enough. The sophistication of calculations considerably increases, for instance, in the problems of gas-oil well perforating, where the geometry of the target and the heterogeneity of its materials play a significant role. It is essential that the interaction is not strictly axisymmetric, and direct numerical modeling requires the application of three-dimensional and probabilistic algorithms.

PII: S0734-743X(01)00123-3

The existence of the said difficulties does not allow the obtaining of the direct problem solution. In this case, it is worthwhile solving the problem stage-by-stage splitting it into separate sub-problems, which can be resolved in one or another way.

In the given paper, the problem concerning the interaction of the shaped charge jet with the target whose thickness does not exceed several jet diameters as well as with a set of such targets, spaced at some distance apart from each other, is considered. The existence of air gaps between such targets lead to additional losses of the jet length due to the erosion of its tip region upon the target perforation, which was first noticed by Brown and Finch [1] and was termed "foreshortening" (forefront shortening).

The aim of the present work is to investigate this problem both computably and experimentally, and to derive semi-empirical formulas enabling the calculation of losses of the jet penetration capability upon separate and spaced-apart targets perforation.

DESCRIPTION AND EXPERIMENTAL CONFIRMATION OF THE JET TIP EROSION EFFECT UPON FINITE THICKNESS TARGET PERFORATION

Upon penetration of the shaped charge jet into the target, jet "wear" takes place, i.e. its energy, mass and length are spent for target perforating. The process of jet 'wear" considerably varies if the target is not semi-infinite, i.e. if its thickness is limited or if the target consists of several layers separated with air gaps. The point is that during the process of the target perforating, the compression of the jet material occurs. Upon leaving the target, the relief of the compressed material takes place leading to considerable expansion of the jet tip having left the target. It is evident that the jet region, expanded radially, has the reduced penetration capability. Brown and Finch [1] noticed the additional loss of the jet length due to the erosion of its tip upon the target perforation. They suggested its accounting by introducing a certain arbitrary shim on the jet way, having no thickness but interacting with the jet in the same manner as does a 10-mm steel plate. In the next papers, Chanteret [2,3] presented a semi-empirical formula to calculate the loss of the jet length due to the foreshortening effect:

$$\frac{\Delta l}{d_j} = 2.9 \cdot \left(1 - e^{-\frac{1.1 \cdot \Delta}{d_j}} \right) \tag{1}$$

The accounting of the foreshortening effect with the use of this empirical formula allowed Chanteret to essentially improve the calculation results for the finite-thickness-target perforation by a jet.

Figure 1 show the X-ray radiograph of copper jet with the radially expanded tip. Upon perforating the 8-mm-thick steel plate at the angle of 90 degrees, the 100-mm-caliber shaped charge jet has the tip velocity of ~ 8.8 km/s. The dimensions of the jet's blurred tip are the following: the length is ~ 9 jet's diameters, the mean diameter is ~5.5 jet's diameters.

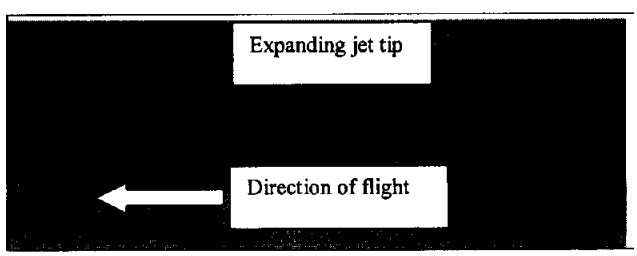

Fig.1. The jet upon perforating the 8-mm-thick steel plate (reconstruction of X-ray radiograph).

The presented X-ray radiograph is the direct experimental evidence of the foreshortening effect existence, though it does not offer enough information for qualitative description. The process's in-depth study can be performed using the multi-frame flash radiography, which requires a great number of experiments with shaped charges. The application of numerical simulations followed by the experimental results calibration, with the limited number of experiments, is a less expensive though a highly effective technique as well. The said investigation technique is employed in the present paper.

HYDROCODE MODELING OF JET INTERACTION WITH THE FINITE-THICKNESS TARGET

To study the effect of various factors (of the jet velocity, of the target material and thickness) on the loss value Δl of the jet length in detail, the numerical simulation of the physical model "target-jet", using the EGAK [4] and SPH [5] 2D-hydrocodes, was carried out. An Eulerian (stationary) computational grid and a concentration method for visualizing of different components are used in EGAK. An irregular moving computational grid and a smoothed particle method [6] are used in SPH. Equations of state, of the Mie-Gruneisen form, and constitutive relations were taken from the material library of the EGAK and SPH codes. Although these two methods are very different, they produced results coinciding with 5% accuracy.

Two bodies represent the «target-jet» model. The 50-mm-diameter and Δ-thick (1; 2; 6; 10 mm) immovable metal (steel or aluminum) "A" plate represents a target. The 4 mm-diameter and l-long flat-faced copper "B" rod, moving with the velocity V (4; 6; 8; 10 km/s), represents a jet. The zone size in the computational grid was chosen so that there were 64 zones across the diameter of the jet. The flow pattern obtained in the EGAK computation for several instants of time are given in Fig.2.

Upon perforating the target and after the arrival of the tip (front end) of the "B" rod at the free surface of the "A" plate, the process of relief of the front region of the "B" rod, compressed in the process of perforation, and of material particles' flying apart begins. This process leads to further reduction of the rod length to the finite value l^*. Subtracting the equivalent (in hydrodynamic approximation) thickness of the perforated target from the length difference $(l\text{-}l^*)$, we will obtain the rod length loss Δl_{FS} due to the foreshortening effect:

$$\Delta l_{FS} = l - l^* - \Delta \cdot \sqrt{\frac{\varrho_A}{\varrho_B}} \tag{2}$$

The results are given in Tables 1-2, where the rod length losses, due to foreshortening, are given for different target materials and thickness as well as on the jet velocity V.

Table 1. Calculated copper rod length losses for steel targets

V, km/s	*u, km/s*	*Code*	*Losses for steel, mm*			
			Δ=1	*Δ=2*	*Δ=6*	*Δ=10*
4	2.08	EGAK	*	5.2	7.8	8.6
6	3.11	EGAK	*	6.4	8.9	10.0
8	4.13	EGAK	5.7	7.3	9.8	10.7
8	4.13	SPH	5.0	6.9	10.1	11.3
10	5.15	EGAK	*	7.9	10.3	10.8

* Values not calculated

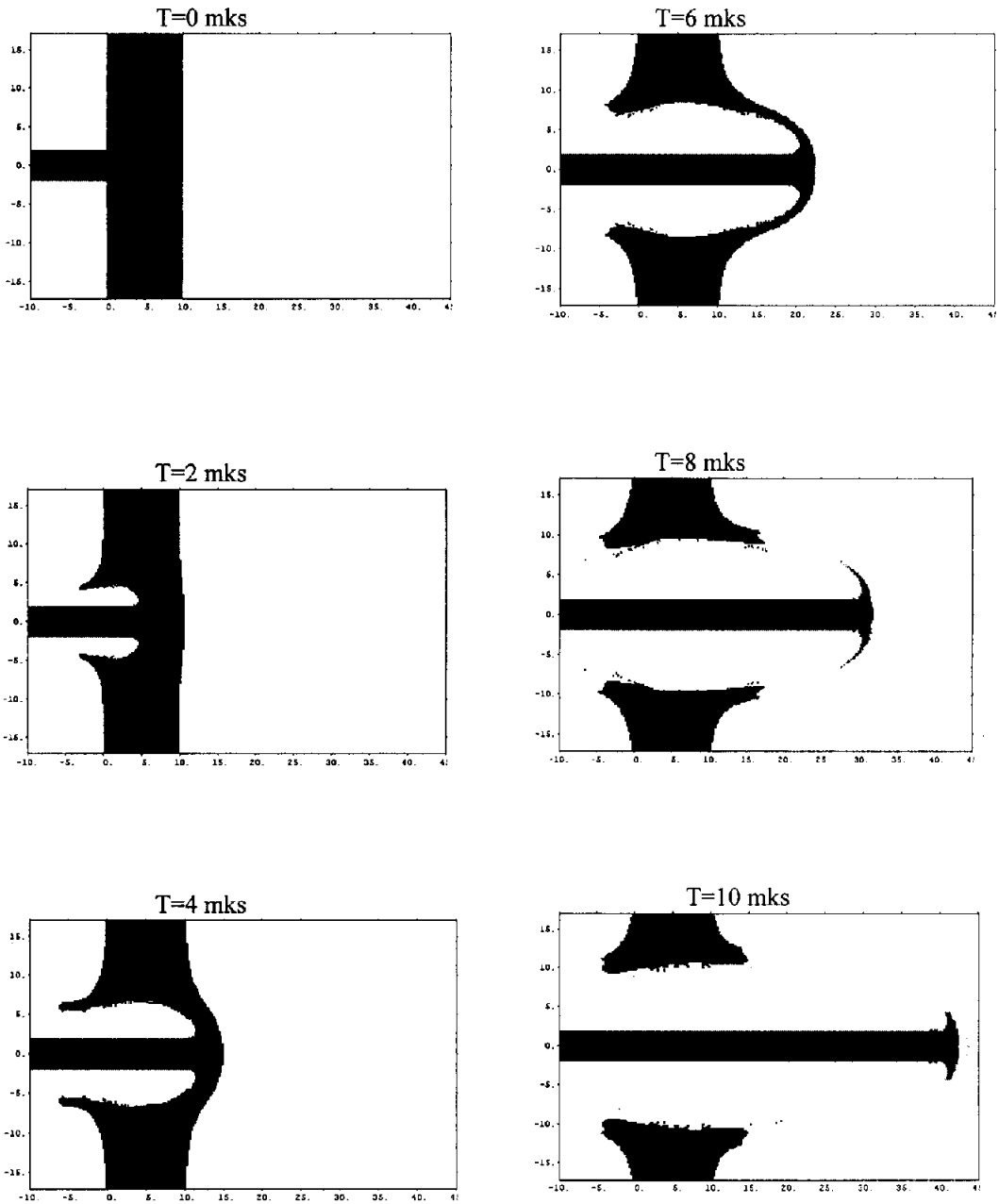

Fig. 2. EGAK hydrocode computation illustrating the additional jet erosion effect on finite thickness plate perforation.

Table 2. Calculated copper rod length losses for aluminum targets

V, km/s	u, km/s	Code	Losses for aluminum, mm		
			Δ=2	Δ=6	Δ=10
4	2.72	EGAK	3.5	4.6	5.1
6	4.05	EGAK	4.6	5.8	6.3
8	5.37	EGAK	5.5	6.6	7.2
8	5.37	SPH	5.3	7.0	7.6
10	6.70	EGAK	6.2	7.0	7.5

With the further processing of the calculation results the attempt was made to derive the semi-empirical formula, including parameters, easily measured in the experiments, namely the target thickness, the jet velocity and diameter, for calculating the jet length losses Δl_{FS}. Of course, this processing is only formal mathematical procedure for searching of better functional form than Chanteret formula.

The dependence of loss on the target thickness Δ was sought in functional form $f(\Delta/(\Delta+d_j))$. The Δl_{FS} results, obtained from the calculations performed using EGAK, were described by the power function, whose base slightly varied depending on the jet velocity, and the exponent variations linearly depended on V (Fig. 3, 4 for specific target materials). Averaging the base value, one can write it as a constant coefficient of the parameter $\Delta/(\Delta+d_j)$. The coefficients of the linear function from V, describing the exponent k (V), can be easily found from the curve of this linear function (Fig. 3, 4).

The final formula is written as:

$$\frac{\Delta l_{FS}}{d_j} = A \cdot \left(\frac{\Delta}{\Delta + d_j} \right)^{B - C \cdot V} \tag{3}$$

where: for steel A=3, B=0.8, C=0.04
for aluminum A=2, B=0.65, C=0.04

Let us see how values Δl_{FS}, derived by using the Svirsky and Chanteret formulas, agree with the calculated data, derived by the two-dimensional EGAK and SPH codes. Since the Chanteret formula was derived only for a steel target and is illustrated by the data for the jet velocity V=8 km/s, then, for comparison, the same initial data should be taken both in the Svirsky formula and in the EGAK and SPH calculations. Fig.5 represents curves $\Delta l_{FS}=f(\Delta)$ obtained in various ways. It is seen that in the range $\Delta \approx 3$-10 mm, all the curves are in satisfactory agreement with each other, in addition, the calculations by the Chanteret formula exhibit the greatest discrepancy with EGAK and SPH.

THE EXPERIMENTAL VERIFICATION OF THE SEMI-EMPIRICAL FORMULA

Let us consider the capabilities of the computation techniques for calculating the perforation losses in the problems of the jet penetration through the spaced targets. Fig.6 represents the layout of the experiments involving the interaction of the 120 mm-caliber shaped charge with the spaced targets.

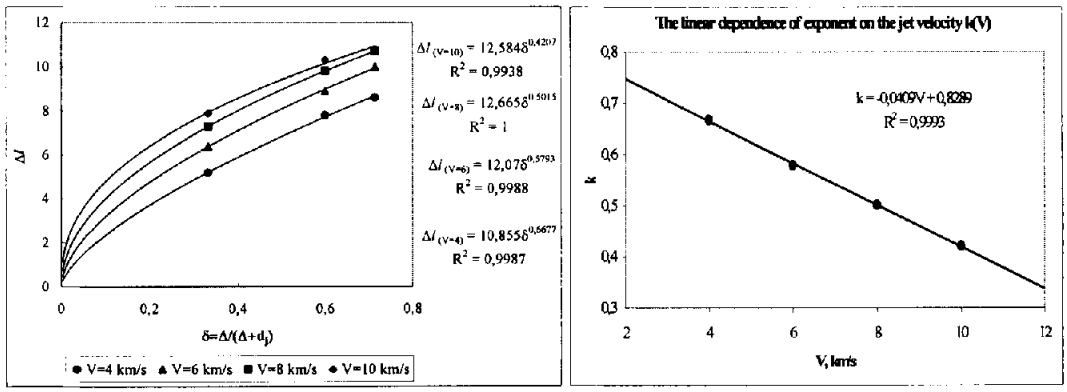

Fig. 3. The computation results approximation for steel targets.

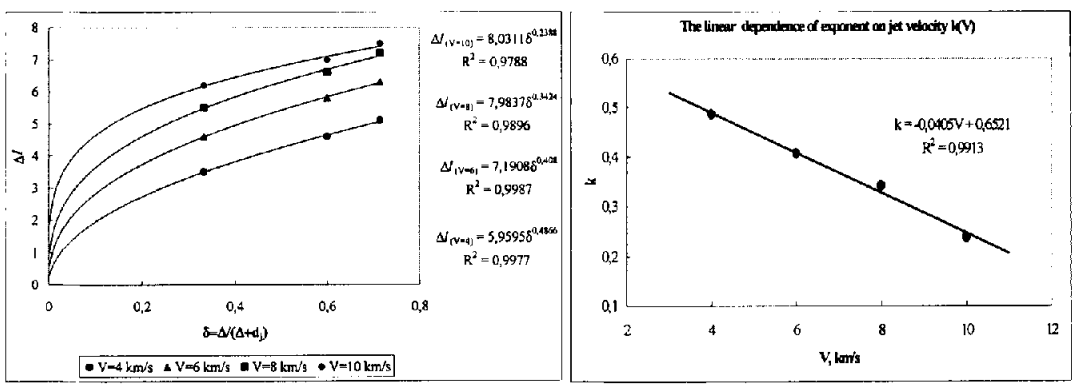

Fig. 4. The computation results approximation for aluminum targets.

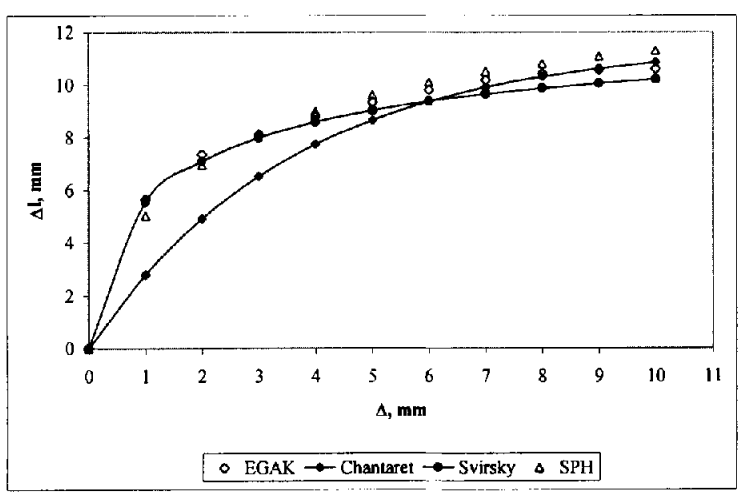

Fig. 5. The comparison of dependencies $\Delta l_{FS}=f(\Delta)$ obtained in various ways (Δ-thickness steel target, V=8 km/s, dj=4 mm.)

Two experiments were performed in the same setup. The jet velocities in different regions and the residual penetration in the last steel target were calculated using the ATOS [4] technique both with accounting of foreshortening effect and without it. The results of calculations and experiments are presented in Table 3, where the indices V_{i0} indicate the jet velocities in front of the target and V_{i1} - are the jet velocities behind the target.

Table 3. Calculated and experimental data for 120-mm shaped charge

V, km/s	*Calculations without foreshortening*	*Calculations with foreshortening*	*Experiment*	
			№1	*№2*
V_{10}	8.8	8.8	8.77	8.8
V_{20}	8.3	8.17	8.15	8.25
V_{21}	7.77	7.64	7.65	7.7
V_{30}	7.77	7.55	7.59	7.62
V_{31}	7.34	7.12	7.16	7.11
V_{40}	7.34	7.04	7.0	7.03
$P^{(*)}$	0,832	0,782	0,802	0,775

(*) - the part from the mean penetration value with the charge affecting the target 4, with no additional targets 1-3 being installed.

As it is seen from Table 3, the calculation values V and P with the accounting of the foreshortening effect are in much better agreement with the experiment than without accounting of this effect.

100 mm-caliber shaped charge results appear more convincing. The layouts of the experiments are represented in Fig.7.

The experimental data on the tip velocity of the shaped charge jet, on residual penetration in the last steel target as well as the calculation data with the accounting of the foreshortening effect and without it are presented in Tables 4,5.

Table 4. Calculated and experimental data for 100-mm shaped charge
(First layout)

V, km/s	*Calculations without foreshortening*	*Calculations with foreshortening*	*Experiment*
V_{10}	9.3	9.3	9.3
V_{20}	9.09	8.82	8.73
V_{30}	8.83	8.41	8.44
$P^{(*)}$	0,900	0,841	0,812

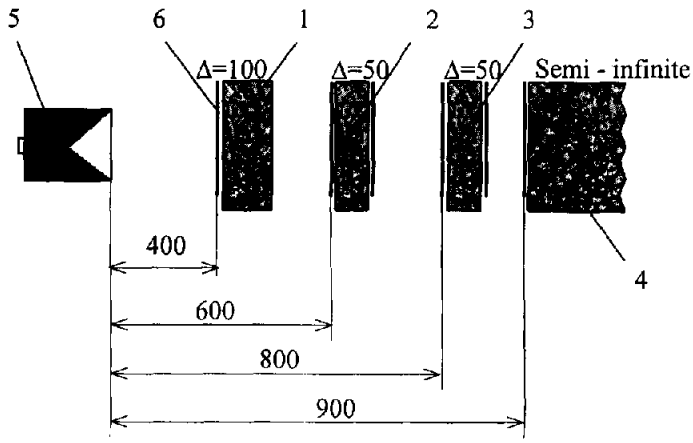

1,2,3,4 – Steel targets
5 – Shaped charge
6 – Contact guides

Fig. 6. The layout of the experiments with 120-mm-caliber shaped charge.

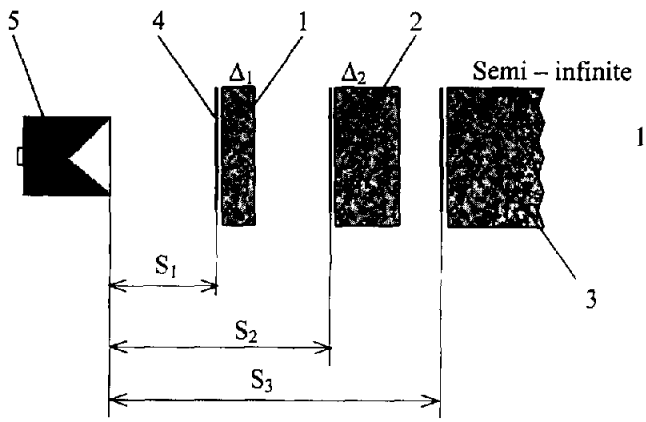

1, 2 – Additional targets
3 – Main steel target
4 – Contact guides
5 – Shaped charge

	S_1	Δ_1	S_2	Δ_2	S_3
Exper. 1	195	8*	475	30**	580
Exper. 2	160	12**	475	50**	675

* - Aluminum
**- Steel

Fig. 7. The layout of the experiments with 100-mm-caliber shaped charge.

Table 5. Calculated and experimental data for 100-mm shaped charge (Second layout)

V, km/s	*Calculations without foreshortening*	*Calculations with foreshortening*	*Experiment*
V_{10}	9.3	9.3	9.3
V_{20}	8.96	8.64	8.64
V_{30}	8.22	7.8	7.42
$P^{(*)}$	0,782	0,718	0,708

(*) - the part from the mean penetration value with the charge affecting the target 3, with no additional targets 1-2 being installed.

Here, as well as in the previous experiments, one can note the satisfactory agreement of the calculations with the experimental data.

Because the proposed formula (3) differs from Chanteret's model primarily in prediction of foreshortening through thin plates ($\Delta/d_j<1$) some additional experiments were made to validate it's significance. Experiments have been performed using 46-mm caliber point initiated shaped charges with 70° opening conical 1-mm thickness copper liner. The main jet parameters are presented in Table 6.

Table 6. Jet parameters

Parameter	*Value*
Virtual origin, B	20 mm
Tip velocity, V	6.6 km/s
Tail velocity, V_t	3.0 km/s
Jet diameter, d_J (at 20-mm standoff)	3.0 mm
Breakup distance, X_b	350 mm

The first three experiments were made to determine the penetration value in RHA target at 100-mm standoff. Then an additional 1-mm thickness steel plate was installed at 20-mm standoff (S_p) and three recurrent experiments were made. The experimental data on residual penetration in the last RHA target are presented in Table 7.

Table 7. RHA penetration data

Exp. No	*Additional plate*	*Penetration, mm*	*Average value*
1	No	160	
2	No	161	157
3	No	150	
4	Yes	120	
5	Yes	129	124
6	Yes	123	

The jet penetrates continuously because the sum of target standoff and penetration value is no greater than the breakup distance. Thus the penetration value is given by Allison-Vitali formula [7,8].

$$P = (S + B) \cdot \left(\left(\frac{V}{V_t} \right)^{\sqrt{\frac{\rho_j}{\rho_t}}} - 1 \right) \tag{4}$$

Using Eq. (4), jet parameters (Table 6) and penetration value P=124 mm (Table 7) allows to calculate the residual jet velocity V_r =5.84 km/s after 1-mm plate perforating and foreshortening. The calculated jet velocity after 1-mm plate perforating only is equal V_p=6.45 km/s. The experimental value for the loss of the jet length due to the foreshortening can be calculate as $\Delta l_{FS} = (S_p+B+\Delta)\cdot(V_p-V_r)/V_p$. Table 8 represents values Δl_{FS} obtained in various ways.

Table 8. Jet length losses Δl_{FS}

Experiment	*Calculation*	
	Chanteret (1)	*Svirsky (3)*
3.88 mm	2.67 mm (-31%)	4.22 mm (+9%)

CONCLUSION

The numerical modeling of the interaction process between the jet and the finite-thickness target was performed. The empirical formula, enabling the calculation of losses Δl_{FS}, using the known initial data, namely the thickness and the target material, the velocity and the diameter of the jet region, interacting with the target, was derived. The results of calculation performed using this formula are in satisfactory agreement with the results of 2-D hydrocode computation and with the Chanteret calculations [3].

The algorithm of additional loss accounting, based on the derived empirical formula, was introduced into the ATOS program for the penetration computation. Its application allowed the calculation of the residue jet penetration after passing through the additional targets, spaced apart, with the deviation of not more than 4% from the values obtained in the experiments.

REFERENCES

[1] J. Brown and D. Finch. The Shaped Charge Jet Attack of Confined and Unconfined Sheet Explosive at Normal Incidence. *Proc. 11th Int. Symp. Ballistics*, Brussels, 9-11 May 1989.

[2] P.Y. Chanteret. On Modelling of Shaped Charges Jet Interaction with Spaced Plates. *Proc. 6th Int. Symp. on Interaction of Nonnuclear Munitions with Structures.* Panama City Beach, 3-7 May 1993.

[3] P.Y. Chanteret. Considerations about the Analytical Modeling of Shaped Charges. *Propellants, Explosives, Pyrotechnics.* 1993; **18**: 337-344.

[4] I.D. Sofronov, R.I. Ilkaev, N.P. Kovalev and O.V. Svirsky. Calculation of shaped charge performance. *Proc. Int. Seminar on Fundamental Problems of Cumulation.* St. Petersburg, July 7-12,1997.

[5] V.V. Bashurov, G.V. Bebenin, A.G. Ioilev. Numerical simulation of rod particles hypervelocity impact effectivity at various attack angles. *Space Forum.* 1996; 1(1-4): 255-262.

[6] L.D. Cloutman. Basic of Smoothed Particle Hydrodynamics. *LLNL Report.* 1990; UCRL-ID-103698.

[7] F.E. Allison and R. Vitali. A New Method of Computing Penetration Variables for Shaped-Charge Jets. *BRL Report.*, January 1963; No 1184.

[8] W. Schwartz. Modified SDM Model for the Calculation of Shaped Charge Hole Profiles. *Propellants, Explosives, Pyrotechnics.* 1994; 19: 192-201.